

Unraveling the correlation between oxide-ion motion and upconversion luminescence in β - $\text{La}_2\text{Mo}_2\text{O}_9\text{:Yb}^{3+}$, Er^{3+} derivatives

Qian He^a, Mingzi Sun^b, Xiao-jun Kuang^c, Bolong Huang^{*b}, Shi Ye^{*a}, Qin-yuan Zhang^a

^a State Key Lab of Luminescent Materials and Devices, and Guangdong Provincial Key Laboratory of Fiber Laser Materials and Applied Techniques, South China University of Technology, Guangzhou 510641, China.

^b Department of Applied Biology and Chemical Technology, The Hong Kong Polytechnic University, Hung Hom, Kowloon, Hong Kong SAR, China

^c Guangxi Ministry-Province Jointly-Constructed Cultivation Base for State Key Laboratory of Processing for Nonferrous Metal and Featured Materials, College of Materials Science and Engineering, Guilin University of Technology, Guilin 541004, China

* Address correspondence-E-mail: msyes@scut.edu.cn, bhuang@polyu.edu.hk

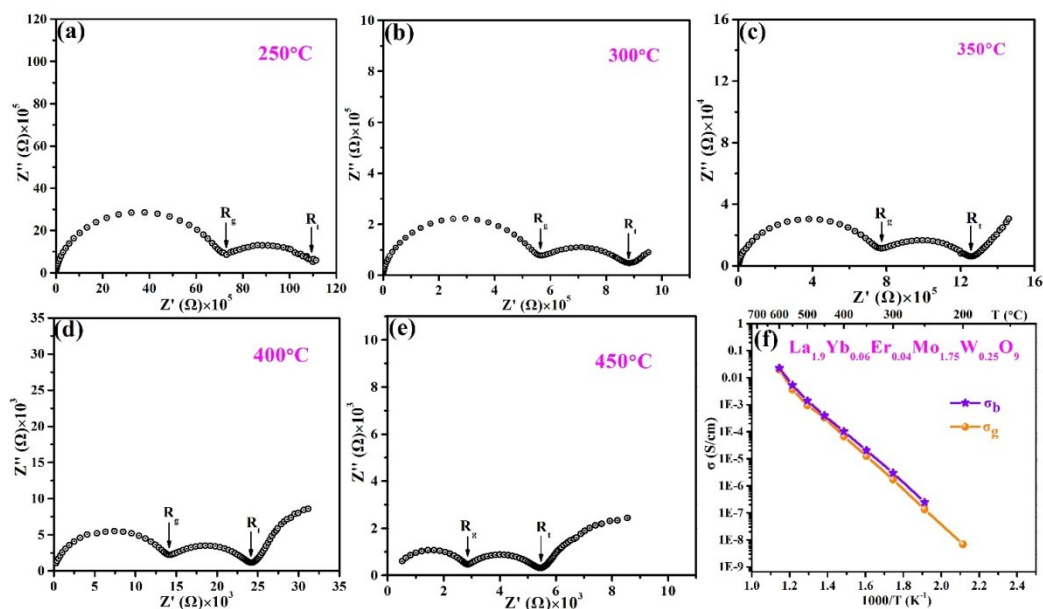


Fig. S1 Complex impedance plots for at (a) 250 °C (b) 300 °C (c) 350 °C (d) 400 °C (e) 450 °C of $\text{La}_{1.9}\text{Yb}_{0.06}\text{Er}_{0.04}\text{Mo}_{1.75}\text{W}_{0.25}\text{O}_9$; (f) Temperature dependency of the grain and boundary electric conductivity of $\text{La}_{1.9}\text{Yb}_{0.06}\text{Er}_{0.04}\text{Mo}_{1.75}\text{W}_{0.25}\text{O}_9$.

It is reported that pure LaGaO_3 perovskite has no oxide-ion conduction, while it is good oxide-ion conductor when doping with Mg^{2+} .^[1-4] Actually, $\text{La}_{0.95}\text{Yb}_{0.03}\text{Er}_{0.02}\text{Ga}_{1-z}\text{Mg}_z\text{O}_3$ material shows no apparent break point for the sample without Mg dopant and those with Mg dopant show break points, as depicted in Fig.S2.

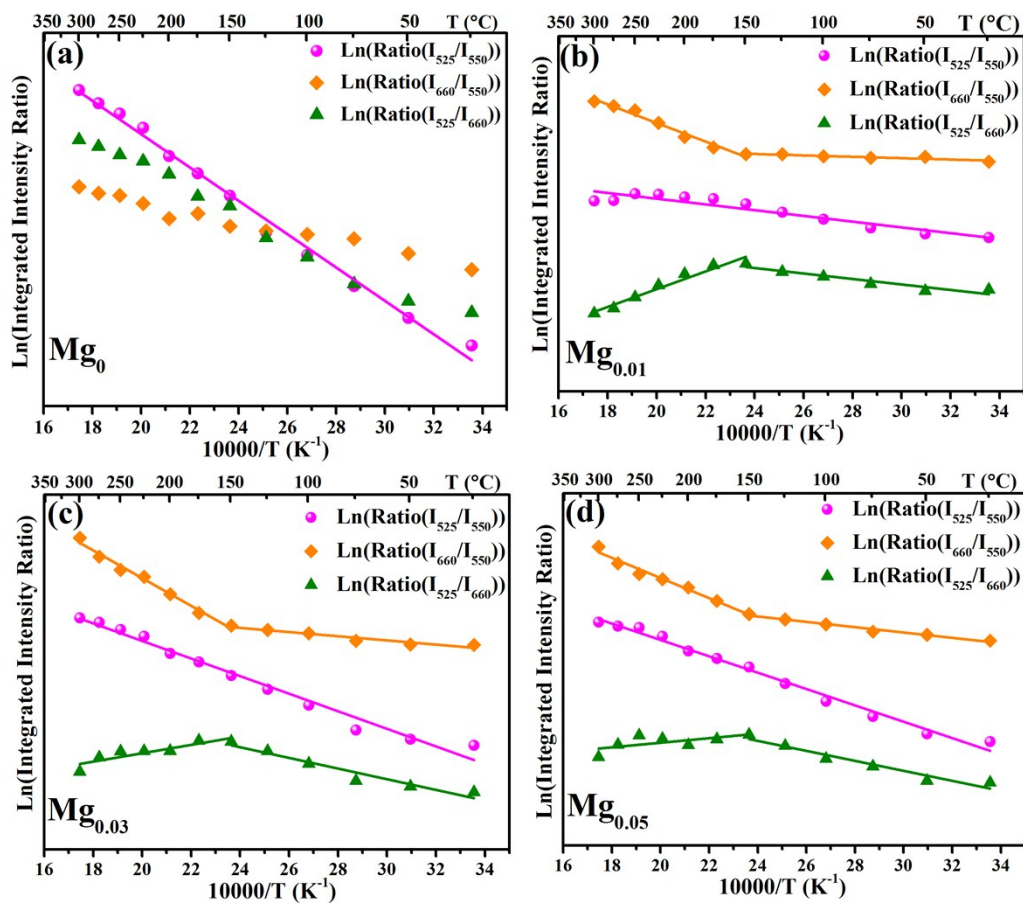


Fig. S2 Logarithmic plot of the intensity ratio of I_{525}/I_{550} ($\text{Ln}(\text{Ratio}(I_{525}/I_{550}))$), I_{660}/I_{550} ($\text{Ln}(\text{Ratio}(I_{660}/I_{550}))$) and I_{525}/I_{660} ($\text{Ln}(\text{Ratio}(I_{525}/I_{660}))$) as a function of inverse absolute temperature of $\text{LaGa}_{1-z}\text{Mg}_z\text{O}_3$ ($z=0, 0.01, 0.03, 0.05$). The lines are fitted.

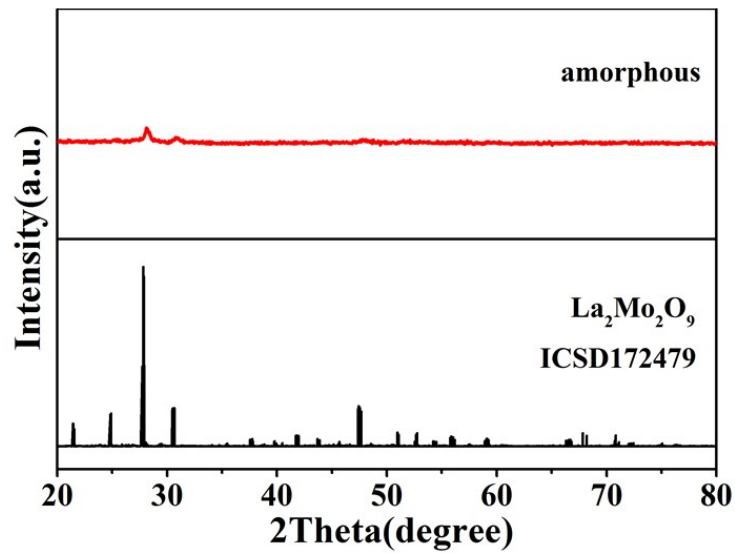


Fig. S3 XRD patterns of amorphous $\text{La}_2\text{O}_3\text{-Yb}_2\text{O}_3\text{-Er}_2\text{O}_3\text{-MoO}_3$, sample recorded at room temperature, along with the reference of monoclinic $\alpha\text{-La}_2\text{Mo}_2\text{O}_9$ (ICSD172479).

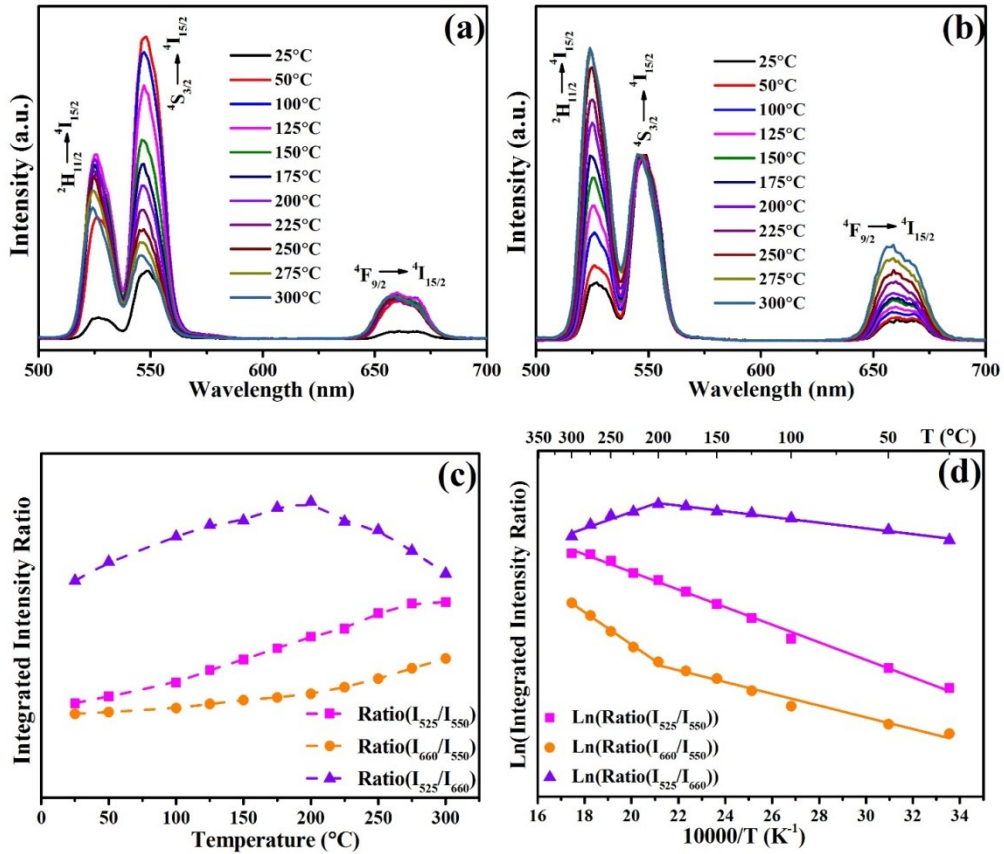


Fig. S4 (a) Temperature-dependent UC emission spectra of amorphous $\text{La}_2\text{O}_3\text{-Yb}_2\text{O}_3\text{-Er}_2\text{O}_3\text{-MoO}_3$ from room temperature to 300°C under excitation of a 980nm laser beam; (b) the same spectra with normalization at 550nm peak. (c) Variations of the integrated UC emission intensity ratios of amorphous $\text{La}_2\text{O}_3\text{-Yb}_2\text{O}_3\text{-Er}_2\text{O}_3\text{-MoO}_3$, i.e., $\text{Ratio}(I_{525}/I_{550})$ (pink square, fitted line), $\text{Ratio}(I_{660}/I_{550})$ (orange circle), and $\text{Ratio}(I_{525}/I_{660})$ (violet up-triangle) (the lines are to guide the eye), with temperature; (d) Lognormal plots of the intensity ratio of I_{525}/I_{550} ($\text{Ln}(\text{Ratio}(I_{525}/I_{550}))$), I_{660}/I_{550} ($\text{Ln}(\text{Ratio}(I_{660}/I_{550}))$) and I_{525}/I_{660} ($\text{Ln}(\text{Ratio}(I_{525}/I_{660}))$) as a function of inverse absolute temperature of amorphous $\text{La}_2\text{O}_3\text{-Yb}_2\text{O}_3\text{-Er}_2\text{O}_3\text{-MoO}_3$, the lines are the fitted.

References

- [1] M. S. Khan, M. S. Islam, D. R. Bates, *J. Phys. Chem. B* **102**, 3099-3104 (1998).
- [2] T. Ishihara, H. Matsuda, Y. Takita, *J. Am. Chem. Soc.* **116**, 3801-3803 (1994).
- [3] T. Inagaki, *Solid State Ionics* **118**, 265-269 (1999).
- [4] T. Ishihara, M. Honda, T. Shibayama, H. Furutani, Y. Takita, *Ionics* **4**, 395-402 (1998)